Supplement to 'Long-run Identification in a Fractionally Integrated System'

Rolf Tschernig* Enzo Weber† Roland Weigand‡

University of Regensburg, Department of Economics,
D-93040 Regensburg, Germany.

September 2010

S1 OVERVIEW

This supplement contains additional material for the paper *Long-run Identification in a Fractionally Integrated System*. It is available from the website of the University of Regensburg Publication Server `http://epub.uni-regensburg.de/16901/` as number 447 in the series Regensburger Diskussionsbeiträge zur Wirtschaftswissenschaft. All equation, figure, and section references with plain numbers refer to items in the main paper. There we consider the bivariate structural fractionally integrated VAR_b (FIVAR_b) model (see equations (12) and (2))

$$\boldsymbol{A}(L_b)\Delta(L;\boldsymbol{d})\boldsymbol{x}_t = \boldsymbol{B}\boldsymbol{\varepsilon}_t, \quad \boldsymbol{\varepsilon}_t \sim IID(\boldsymbol{0};\boldsymbol{I}). \tag{S1}$$

Section S2 contains an algorithm to compute the impact matrix $\boldsymbol{B}$ under finite-horizon restrictions that are introduced in Section 2.3. Section S3 clarifies the relation between long-run and finite-horizon identification restrictions and Section S4 provides more details about the Monte Carlo study of Section 3.4, in particular Monte Carlo distributions for all impulse response functions as well as results on processes with four lags.

S2 COMPUTATION OF IMPACT MATRIX OF FINITE-HORIZON RESTRICTIONS

In the following we discuss the computation of the impact matrix $\boldsymbol{B}$ satisfying the finite-horizon identifying restrictions FIN1 (17), FIN2 (18) and FIN3 (19) that are defined in the main

*Phone: +49 (0) 941 943 2736, Mail: Rolf.Tschernig@wiwi.uni-regensburg.de
†Phone: +49 (0) 941 943 1952, Mail: Enzo.Weber@wiwi.uni-regensburg.de
‡Phone: +49 (0) 941 943 2738, Mail: Roland.Weigand@wiwi.uni-regensburg.de

paper in analogy to Faust (1998).

Note that in the given setup any identification scheme (up to sign differences) can be indexed by a single number. Due to the assumption $\mathrm{Var}(\boldsymbol{\varepsilon}_t) = \boldsymbol{I}$, we have $\boldsymbol{B}\boldsymbol{B}' = \boldsymbol{\Omega}$. Let $\boldsymbol{P}$ be a lower triangular matrix, obtained from a Cholesky decomposition of $\boldsymbol{\Omega}$, such that $\boldsymbol{P}\boldsymbol{P}' = \boldsymbol{\Omega}$. Any feasible impact matrix $\boldsymbol{B}$ is given by $\boldsymbol{P}\boldsymbol{D}$ with $\boldsymbol{D}\boldsymbol{D}' = \boldsymbol{I}$ since then $\boldsymbol{B}\boldsymbol{B}' = \boldsymbol{P}\boldsymbol{D}\boldsymbol{D}'\boldsymbol{P}' = \boldsymbol{P}\boldsymbol{P}' = \boldsymbol{\Omega}$. The orthonormality of $\boldsymbol{D}$ implies that a single number $\beta \in [-1; 1]$ determines $\boldsymbol{D}$ completely (up to sign). Here we use

$$\boldsymbol{B} = \boldsymbol{P}\boldsymbol{D} = \begin{pmatrix} p_{11} & 0 \\ p_{21} & p_{22} \end{pmatrix} \begin{pmatrix} \sqrt{1-\beta^2} & \beta \\ -\beta & \sqrt{1-\beta^2} \end{pmatrix}. \tag{S2}$$

Thus, by choosing $\beta \in [-1; 1]$ the impact matrix $\boldsymbol{B}$ is completely specified.

First, observe that for any h the forecast error covariance matrix of $\boldsymbol{x}_{t+h}$ is independent of β since $\boldsymbol{\Omega} = \boldsymbol{B}\boldsymbol{B}'$ is. To see this, let denote $\boldsymbol{\Phi}(L) := \Delta(L; -\boldsymbol{d})\boldsymbol{A}(L_b)^{-1}$, which is independent of $\boldsymbol{B}$. Then, recalling $\boldsymbol{x}_t = \boldsymbol{\Theta}(L)\boldsymbol{\varepsilon}_t$,

$$\mathrm{Var}_t\left(\boldsymbol{x}_{t+h}\right) = \sum_{j=0}^{h-1} \boldsymbol{\Theta}_j \boldsymbol{\Theta}_j' = \sum_{j=0}^{h-1} \boldsymbol{\Phi}_j \boldsymbol{B}\boldsymbol{B}' \boldsymbol{\Phi}_j' = \sum_{j=0}^{h-1} \boldsymbol{\Phi}_j \boldsymbol{\Omega} \boldsymbol{\Phi}_j' \tag{S3}$$

and therefore $\mathrm{Var}_t\left(x_{s,t+h}\right)$, $s = 1, 2$, given by (15) is independent of β as well.

Now consider the variance component in (15) that is attributed to shock k. Denoting the unit basis vector with 1 in the ith row by $\boldsymbol{e}_i$, the impulse response of variable s to shock k is given by

$$\theta_{sk,j} = \boldsymbol{e}_s' \boldsymbol{\Phi}_j \boldsymbol{P}\boldsymbol{D}\boldsymbol{e}_k = \boldsymbol{e}_s' \boldsymbol{\Phi}_j \boldsymbol{P}\boldsymbol{d}_k, \quad \text{where } \boldsymbol{d}_1 = \begin{pmatrix} \sqrt{1-\beta^2} \\ -\beta \end{pmatrix}, \quad \boldsymbol{d}_2 = \begin{pmatrix} \beta \\ \sqrt{1-\beta^2} \end{pmatrix}.$$

By construction $\boldsymbol{d}_k$, $k = 1, 2$, are orthonormal vectors that exclusively depend on β. The h-step forecast variance of variable s due to the kth shock and its share $\omega_{sk,h}$ (16) are then obtained by

$$\omega_{sk,h} = \frac{\sum_{j=0}^{h-1} \boldsymbol{d}_k' \boldsymbol{P}' \boldsymbol{\Phi}_j' \boldsymbol{e}_s \boldsymbol{e}_s' \boldsymbol{\Phi}_j \boldsymbol{P} \boldsymbol{d}_k}{\mathrm{Var}_t(x_{s,t+h})} = \boldsymbol{d}_k' \boldsymbol{V}_{sh} \boldsymbol{d}_k, \quad \text{where } \boldsymbol{V}_{sh} = \frac{\sum_{j=0}^{h-1} \boldsymbol{P}' \boldsymbol{\Phi}_j' \boldsymbol{e}_s \boldsymbol{e}_s' \boldsymbol{\Phi}_j \boldsymbol{P}}{\mathrm{Var}_t(x_{s,t+h})}. \tag{S4}$$

Since $\boldsymbol{V}_{sh}$ is positive semidefinite and symmetric by construction, it can be represented as (Lütkepohl 1996, Section 9.13.3, Result (2))

$$\boldsymbol{V}_{sh} = \lambda_1 \boldsymbol{v}_1 \boldsymbol{v}_1' + \lambda_2 \boldsymbol{v}_2 \boldsymbol{v}_2', \tag{S5}$$

where λ_k and $\boldsymbol{v}_k$ denote the nonnegative eigenvalues and corresponding orthonormal eigenvectors, respectively.

Now observe that inserting (S5) into (S4) delivers $\omega_{sk,h} = \lambda_1 (\boldsymbol{d}_k' \boldsymbol{v}_1)^2 + \lambda_2 (\boldsymbol{d}_k' \boldsymbol{v}_2)^2$, $0 \leq (\boldsymbol{d}_k' \boldsymbol{v}_1)^2, (\boldsymbol{d}_k' \boldsymbol{v}_2)^2 \leq 1$, where the latter property follows from orthonormality of $\boldsymbol{d}_k, \boldsymbol{v}_1, \boldsymbol{v}_2$. Since both eigenvalues are nonnegative, the minimum of $\omega_{sk,h}$ is obtained and thus restriction FIN1

(17) fulfilled if one chooses $\boldsymbol{d}_k = \boldsymbol{v}_1, \boldsymbol{d}_{k'} = \boldsymbol{v}_2$ if $\lambda_1 \leq \lambda_2$ and $\boldsymbol{d}_k = \boldsymbol{v}_2, \boldsymbol{d}_{k'} = \boldsymbol{v}_1$ otherwise. Finally, obtain the impact matrix as $\boldsymbol{B} = \boldsymbol{P}\boldsymbol{D}$.

To impose FIN2 (18), $\boldsymbol{B}$ is analogously computed by averaging $\bar{\boldsymbol{V}}_s = \frac{1}{u-l+1}\sum_{j=l}^{u} \boldsymbol{V}_{sj}$, and again going through the steps above.

To ensure condition (19), replace $\boldsymbol{V}_{sh}$ in (S4) by $\frac{\sum_{j=l}^{h-1} \boldsymbol{P}'\boldsymbol{\Phi}_j' \boldsymbol{e}_s \boldsymbol{e}_s' \boldsymbol{\Phi}_j \boldsymbol{P}}{\mathrm{Var}_t(x_{s,t+h})}$ and go through the steps above.

S3 RELATION BETWEEN LONG-RUN AND FINITE-HORIZON RESTRICTIONS

We show for the case $d_1 > 0.5$ that identification by the restrictions FIN1 (17) and FIN2 (18) yield the same result as LRR (7) if $h \to \infty$, while FIN3 (19) is asymptotically equivalent for $u \to \infty$.

For $\beta \in [-1; 1]$ implicitly defined by (S2) write $\theta_{12}(L; \beta) = \theta_{12,0}(\beta) + \theta_{12,1}(\beta)L + \theta_{12,2}(\beta)L^2 + \ldots$. Then for large j one has $\theta_{12,j}(\beta) = \frac{\xi_{12}(1;\beta)}{\Gamma(d_1)} j^{d_1-1} + o(j^{d_1-1})$, as shown by Chung (2001, Corollary 2) in the standard FIVAR setup. The same applies in the FIVAR$_b$ model since then $\theta_{12}(L; \beta) = \xi_{12}(1; \beta)\Delta^{-d_1} + \theta^*_{12}(L; \beta)$ with $\theta^*_{12}(L; \beta) := \Delta^{b-d_1}\xi^*_{12}(L_b; \beta)$. Here $\theta^*_{12,j}(\beta)$ are the MA coefficients of an I$(d_1 - b)$ process, which are hence bounded of order $O(j^{d_1-b-1}) = o(j^{d_1-1})$. Hence for the squared impulse responses we have $\theta^2_{12,j}(\beta) = \frac{\xi_{12}(1;\beta)^2}{\Gamma(d_1)^2} j^{2d_1-2} + o(j^{2d_1-2})$. Further note that $\mathrm{Var}_t(x_{1,t+h}) = Ch^{2d_1-1} + o(h^{2d_1-1})$ with $C > 0$, see Schotman et al. (2008, eq. A20). By (S3) $\mathrm{Var}_t(x_{1,t+h})$ does not depend on β and neither does C.

Define

$$X_h(\beta) := h^{1-2d_1} \sum_{j=1}^{h} \theta^2_{12,j}(\beta),$$

$$Y_h := h^{1-2d_1} \mathrm{Var}_t(x_{1,t+h})$$

and likewise $Y_\infty := \lim_{h\to\infty} Y_h > 0$ which is related to C. By Schotman et al. (2008, eq. A19) $\sum_{i=1}^{k} i^a k^{-(a+1)} \overset{k\to\infty}{\longrightarrow} (a+1)^{-1}$ and therefore

$$\lim_{h\to\infty} X_h(\beta) = \frac{\xi_{12}(1;\beta)^2}{\Gamma(d_1)^2} \frac{1}{2d_1 - 1}. \tag{S6}$$

Hence the objective of FIN1 (17) satisfies

$$\omega_{12,h} = \frac{X_h(\beta)}{Y_h} \longrightarrow \frac{\xi_{12}(1;\beta)^2}{\Gamma(d_1)^2 Y_\infty} \frac{1}{2d_1 - 1} \quad \text{as } h \to \infty. \tag{S7}$$

The latter expression is minimized by taking β satisfying LRR (7) because then $\xi_{12}(1;\beta)^2 = 0$ while the other terms are strictly positive in any case (since $d_1 > 0.5$ and nonstationarity of x_{1t} is assumed). The same result holds for FIN3 (19) with fixed l and $h \to \infty$ because $h^{1-2d_1}\sum_{j=1}^{h} \theta^2_{12,j}(\beta) - h^{1-2d_1}\sum_{j=l}^{h} \theta^2_{12,j}(\beta) = h^{1-2d_1}\sum_{j=1}^{l-1} \theta^2_{12,j}(\beta) = O(h^{1-2d_1})$.

We now turn to FIN2 (18). Here we have $(u-l+1)^{-1}\sum_{h=l}^{u}\omega_{12,h} = u^{-1}\sum_{h=1}^{u}\omega_{12,h}+O(u^{-1})$ and hence as $u\to\infty$ inclusion of $\omega_{12,h}$ for $h=1,\dots,l$ is negligible. Instead of FIN2 (18) we can therefore consider

$$\frac{1}{u}\sum_{h=1}^{u}\omega_{12,h} = \frac{1}{u}\sum_{h=1}^{u}\frac{X_h(\beta)}{Y_h}$$

Hence, using (S7) and Davidson (1994, Theorem 2.26), we find

$$\lim_{u\to\infty}\frac{1}{u-l+1}\sum_{h=l}^{u}\omega_{12,h} = \lim_{u\to\infty}\frac{1}{u}\sum_{h=1}^{u}\omega_{12,h} = \frac{\xi_{12}(1;\beta)^2}{\Gamma(d_1)^2 Y_\infty}\frac{1}{2d_1-1}$$

which is again minimized for $\xi_{12}(1;\beta)=0$.

For the parameters of the stylized FIVAR$_b$ process

$$\left[\begin{pmatrix}1&0\\0&1\end{pmatrix}-\begin{pmatrix}0&-0.5\\0&0.5\end{pmatrix}L_b\right]\begin{pmatrix}\Delta^{0.7}&0\\0&\Delta^{1.7}\end{pmatrix}\boldsymbol{x}_t=\boldsymbol{u}_t,\quad \boldsymbol{\Omega}=\begin{pmatrix}1&0\\0&1\end{pmatrix}. \tag{S8}$$

we want to evaluate the proximity of different identifying conditions for various values of u and h. Figure S1 gives the implied impulse responses of shocks identified by (18) and (19) with different choices of l and u. We see that with growing u both finite horizon restrictions yield results that get closer to LRR (7). This is most rapidly the case for restriction (19), where short-run influence is kept apart from the objective function for $l\geq 0$. For larger values of l the objective of both restrictions is based on longer horizons and hence we get closer to LRR.

S4 MONTE CARLO RESULTS

This section provides more details about the Monte Carlo study of Section 3.4, in particular Monte Carlo distributions for all impulse response functions as well as results on processes with four lags. For each data generating mechanism 5000 realizations are simulated with Gaussian innovations and sample size $n=250$ as in the empirical analysis. The parameters are estimated by assuming either an IVAR(1,1), IVAR(1,2) or FIVAR$_{d_1}$ model with LRR (7) imposed. For a description of the estimation procedure see Section 3.4. There, only results for the estimation of the impulse responses $\theta_{12,h}$, $h=0,1,\dots,60$ are presented where data are generated either by a FIVAR$_b$ process or an IVAR(1,1) process each with one lag.

In the following we present i) for the mentioned setup the estimation results for all impulse responses $\theta_{sk,h}$, $s,k=1,2$, ii) results on realizations generated by a FIVAR$_b$ and an IVAR(1,1) process each with four lags, iii) estimation results for the latter generating models with misspecified lag length. The data generating processes considered are:

FIVAR$_b$1. This specification matches integration orders, the reduced form error covariance matrix and $\boldsymbol{A}(1)$ matrix of a FIVAR$_{d_1}$ model with four lags fitted to GDP and prices in Section

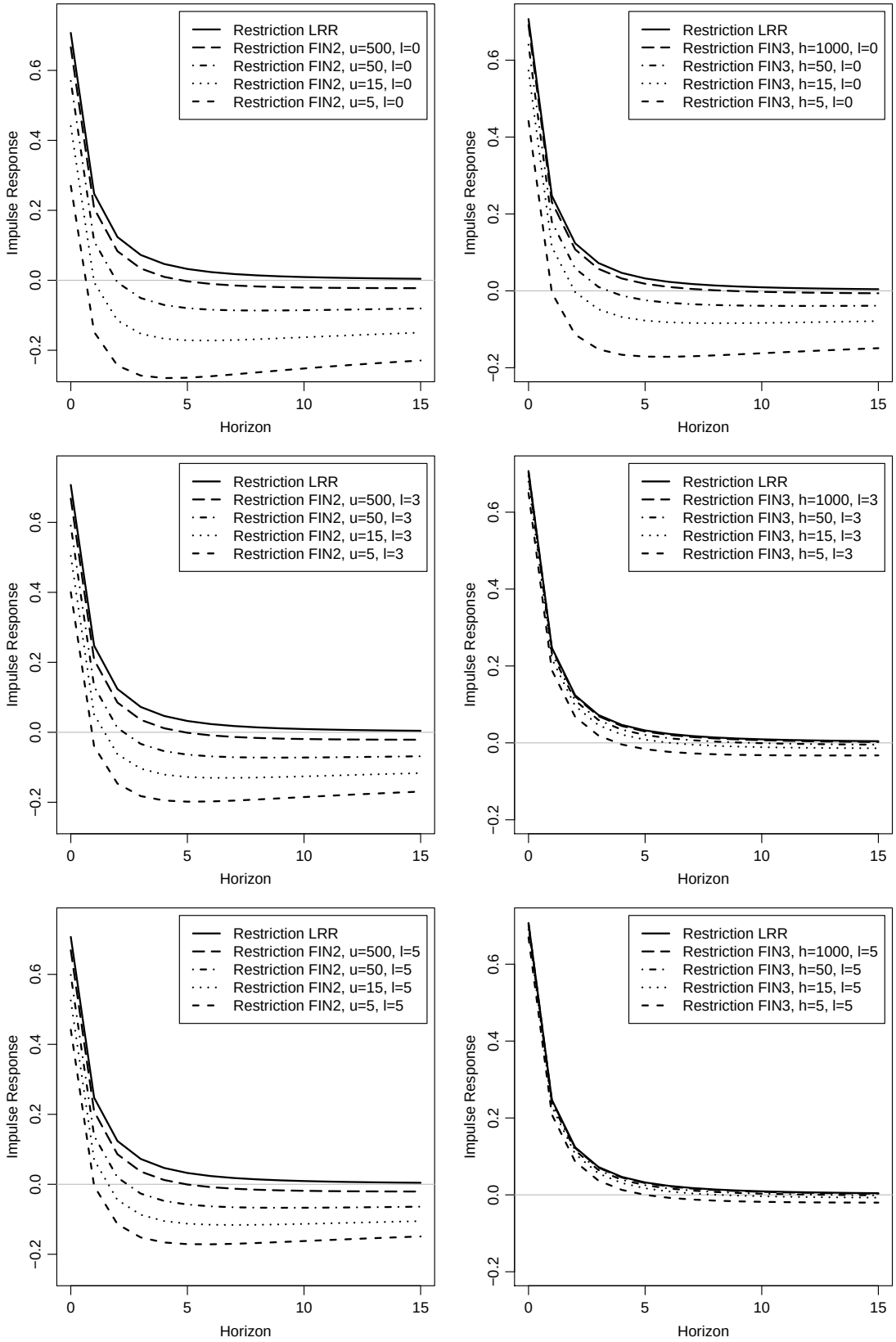

Figure S1: Impulse response of the first variable to the second shock, obtained by process (S8) and imposing LRR and either FIN2 (left) or FIN3 (right) with different values of u and l. FIN1 corresponds to the upper right graph (FIN3 with $l = 0$).

4.2 such that the impact matrix $\boldsymbol{B}$ and the long-run characteristics given by the first term in the Granger representation (13) are the same (cf. (24))

$$\left[\begin{pmatrix}1&0\\0&1\end{pmatrix}-\begin{pmatrix}0.5&-1.5\\0.18&0.2\end{pmatrix}L_{0.83}\right]\begin{pmatrix}\Delta^{0.83}&0\\0&\Delta^{1.77}\end{pmatrix}\boldsymbol{x}_t=\boldsymbol{u}_t,\quad \boldsymbol{\Omega}=\begin{pmatrix}6.9&-0.11\\-0.11&0.71\end{pmatrix}. \tag{S9}$$

FIVAR$_b$4. This specification corresponds to the estimated FIVAR$_{d_1}$ model with four lags fitted to GDP and prices in Section 4.2

$$\left[\begin{pmatrix}1&0\\0&1\end{pmatrix}-\begin{pmatrix}0.56&0.33\\0.04&-0.46\end{pmatrix}L_{0.83}-\begin{pmatrix}0.16&0.17\\0&-0.13\end{pmatrix}L_{0.83}^2-\begin{pmatrix}-0.19&-0.86\\0.04&-0.05\end{pmatrix}L_{0.83}^3 - \begin{pmatrix}-0.02&0.09\\-1.14&0.44\end{pmatrix}L_{0.83}^4\right]\begin{pmatrix}\Delta^{0.83}&0\\0&\Delta^{1.77}\end{pmatrix}\boldsymbol{x}_t=\boldsymbol{u}_t,\quad \boldsymbol{\Omega}=\begin{pmatrix}6.9&-0.11\\-0.11&0.71\end{pmatrix}. \tag{S10}$$

IVAR1. This specification matches the reduced form error covariance matrix and $\boldsymbol{A}(1)$ matrix of an IVAR(1,1) model with four lags fitted to GDP and prices in Section 4.2 (cf. (25))

$$\left[\begin{pmatrix}1&0\\0&1\end{pmatrix}-\begin{pmatrix}0.26&-0.24\\0.12&0.96\end{pmatrix}L\right]\begin{pmatrix}\Delta&0\\0&\Delta\end{pmatrix}\boldsymbol{x}_t=\boldsymbol{u}_t,\quad \boldsymbol{\Omega}=\begin{pmatrix}7.4&-0.2\\-0.2&0.77\end{pmatrix}. \tag{S11}$$

IVAR4. This specification corresponds to the estimated IVAR(1,1) model with four lags fitted to GDP and prices in Section 4.2

$$\left[\begin{pmatrix}1&0\\0&1\end{pmatrix}-\begin{pmatrix}0.3&0.26\\0.02&0.41\end{pmatrix}L-\begin{pmatrix}0.12&-0.05\\0&0.28\end{pmatrix}L^2-\begin{pmatrix}-0.08&-0.45\\0.03&0.07\end{pmatrix}L^3 - \begin{pmatrix}-0.08&0\\0.06&0.2\end{pmatrix}L^4\right]\begin{pmatrix}\Delta&0\\0&\Delta\end{pmatrix}\boldsymbol{x}_t=\boldsymbol{u}_t,\quad \boldsymbol{\Omega}=\begin{pmatrix}7.4&-0.2\\-0.2&0.77\end{pmatrix}. \tag{S12}$$

Simulation results can be found in Figures S2 to S21. Figures S2, S6, S12 and S16 contain boxplots of the estimated impact coefficients based on all realizations of each data generating process. The other figures display boxplots of estimated impulse responses up to horizon 60.

Outcomes for the FIVAR$_b$1 process can be found in Figures S2 to S5. Impact coefficients of both the IVAR(1,1) and IVAR(1,2) are seriously misleading and sampling uncertainty is largest for the IVAR(1,1) model, see Figure S2. Inspection of estimated impulse responses for the IVAR(1,1) specification in Figure S3 suggests that the estimated negative effect of LRUS to prices in the IVAR(1,1) model displayed in Figure 10 may be due to misspecification. On the other hand, a misspecified IVAR(1,2) model may overstate the positive impact of LRRS on prices, compare Figures S4 and 11. Note that the IVAR(1,1) overstates while the IVAR(1,2) understates the effect of LRRS to GDP in intermediate horizons. The correctly specified FIVAR$_{d_1}$ model performs quite well according to Figure S5.

Most of these comments apply to the results based on the FIVAR$_b$4 specification as well if the lag length is correctly specified, see Figures S6 to S9. Not surprisingly, there is higher sampling uncertainty for all estimators because more parameters have to be estimated. Misspecifying the lag length with $p = 1$ shifts estimated impulse responses for the first variable to LRRS towards zero, see Figures S10 and S11, so that the bias of the IVAR(1,1) based estimates diminishes while the FIVAR$_b$ based estimates become heavily biased. Thus, misspecifying the lag order can also have severe effects on the impulse response estimation.

If the true process is the one-lag IVAR1, see Figures S12 to S15, only the IVAR(1,2) model is misspecified. Over-differencing has a very severe impact on impact coefficients and impulse response estimates. This is the effect of losing low-frequency information (see Gospodinov et al. 2010). Responses of the first variable to the LRRS cannot be captured by this specification at all. Estimating $\boldsymbol{d}$ in the FIVAR$_{d_1}$ model inflates variance, but not too much, as the interquartile ranges (box widths) suggest. We also observed that d_2 is precisely estimated despite the largest autoregressive root being close to the unit circle.

The IVAR4 setup contains four lags and Figures S16 to S19 display the simulation results. We find that the estimation uncertainty of the parameters based on the FIVAR$_{d_1}$ specification gets rather large. This may also be caused by a bimodal distribution of $\hat{d}_2$ that we observed in the simulations, where one mode is at $d_2 \approx 1.8$ rather than $d = 1$. This finding is not so surprising in light of the largest root of $\boldsymbol{A}(L)$ close to 1 and d estimates much larger than 1 erroneously capture the autoregressive dynamics. This possibility has to be taken into account in the empirical analysis. In the IVAR4 setup, lag order misspecification has again serious consequences, see Figures S20 and S21.

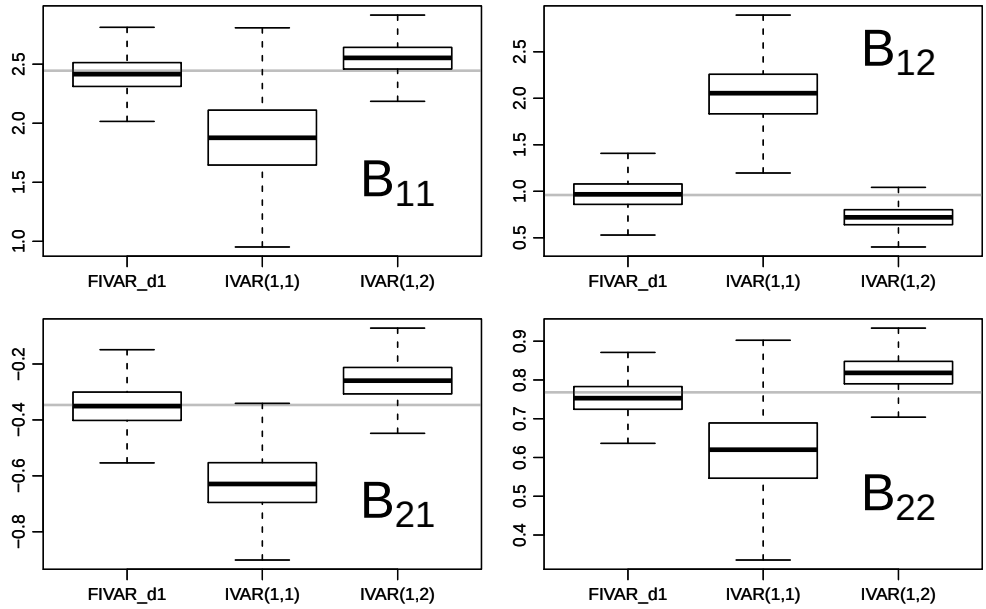

Figure S2: Boxplots of estimated impact coefficients. The true process is given by FIVAR$_b$1 (S9) of which 5000 replications with 250 observations were drawn.

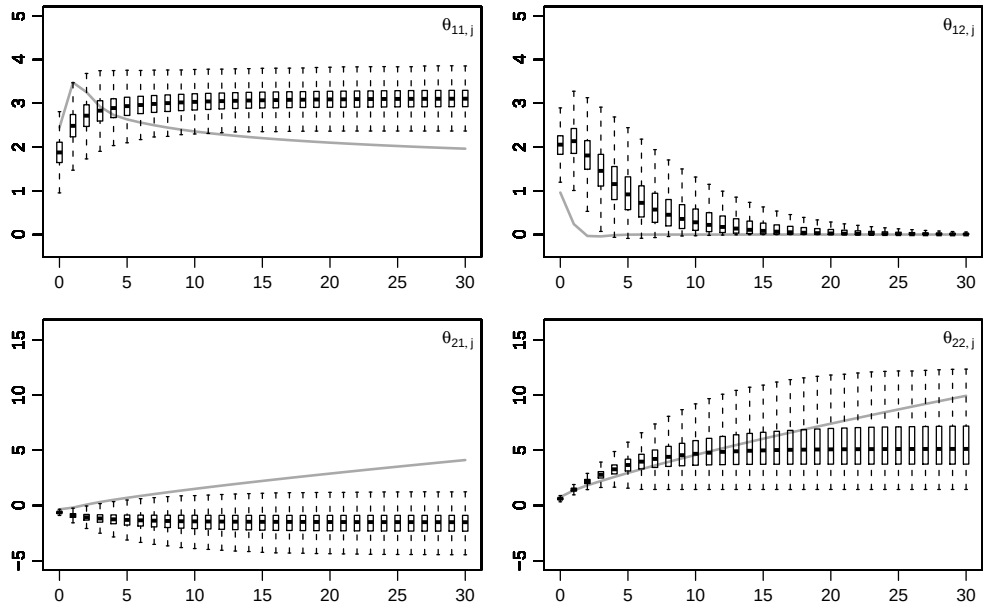

Figure S3: Boxplots of estimated impulse responses based on an IVAR(1,1) model with one lag. The solid line shows the true impulse responses from the FIVAR$_b$1 process (S9) of which 5000 replications with 250 observations were drawn.

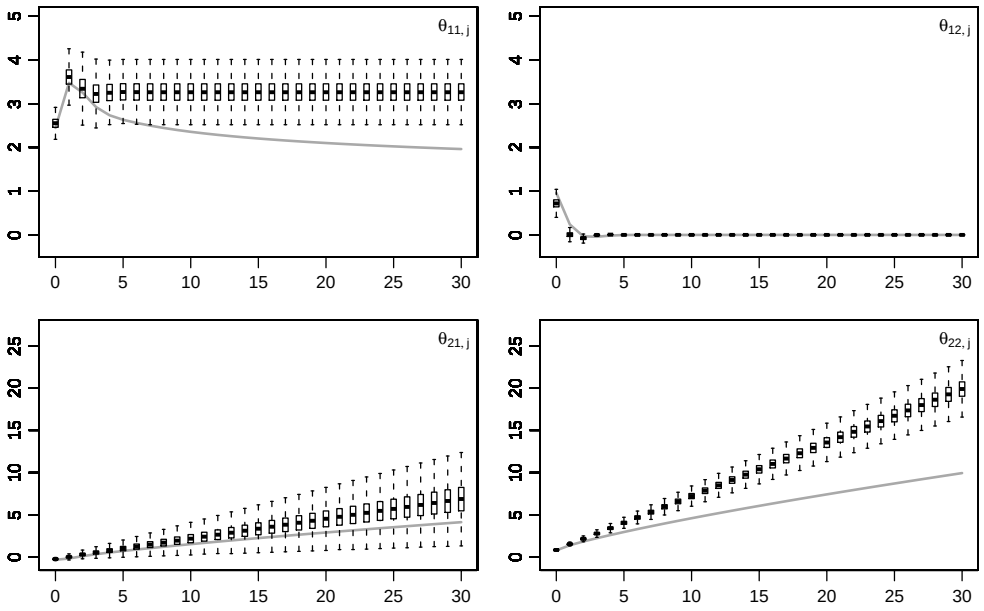

Figure S4: Boxplots of estimated impulse responses based on an IVAR(1,2) model with one lag. The solid line shows the true impulse responses from the FIVAR$_b$1 process (S9) of which 5000 replications with 250 observations were drawn.

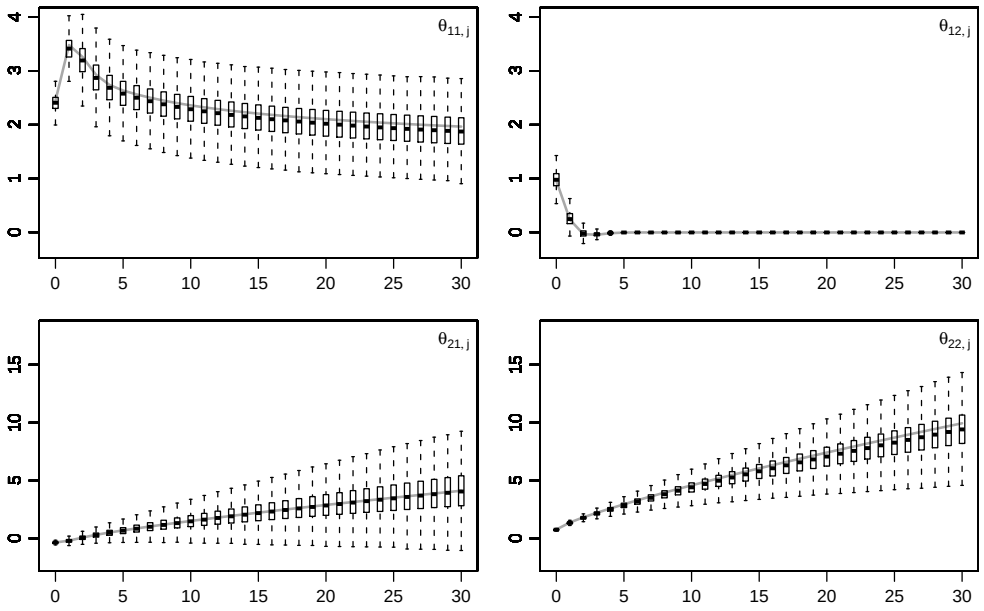

Figure S5: Boxplots of estimated impulse responses based on a FIVAR$_{d_1}$ model with one lag. The solid line shows the true impulse responses from the FIVAR$_b$1 process (S9) of which 5000 replications with 250 observations were drawn.

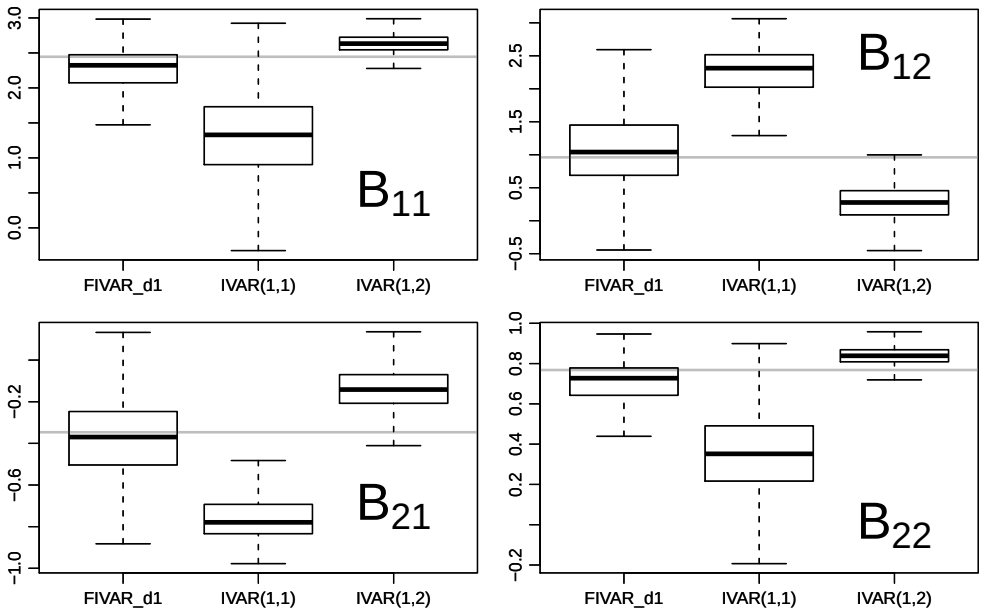

Figure S6: Boxplots of estimated impact coefficients. The true process is given by FIVAR$_b$4 (S10) of which 5000 replications with 250 observations were drawn.

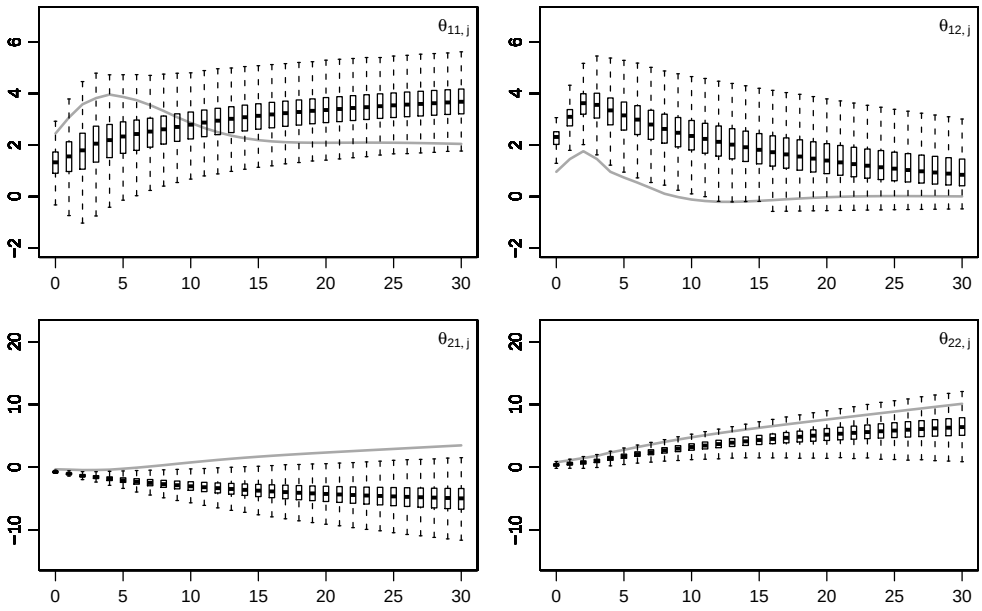

Figure S7: Boxplots of estimated impulse responses based on an IVAR(1,1) model with four lags. The solid line shows the true impulse responses from the FIVAR$_b$4 process (S10) of which 5000 replications with 250 observations were drawn

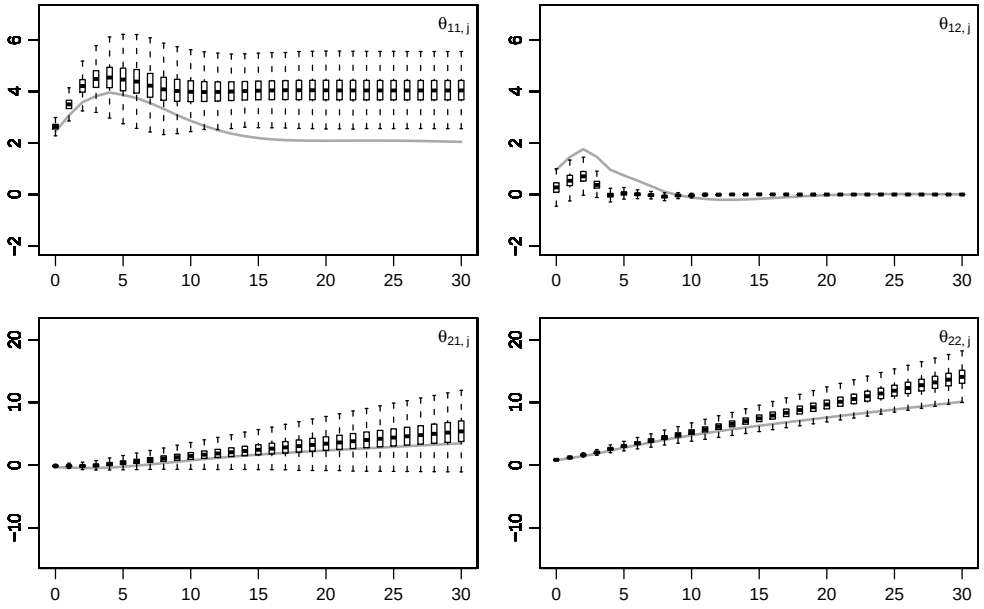

Figure S8: Boxplots of estimated impulse responses based on an IVAR(1,2) model with four lags. The solid line shows the true impulse responses from the FIVAR$_b$4 process (S10) of which 5000 replications with 250 observations were drawn

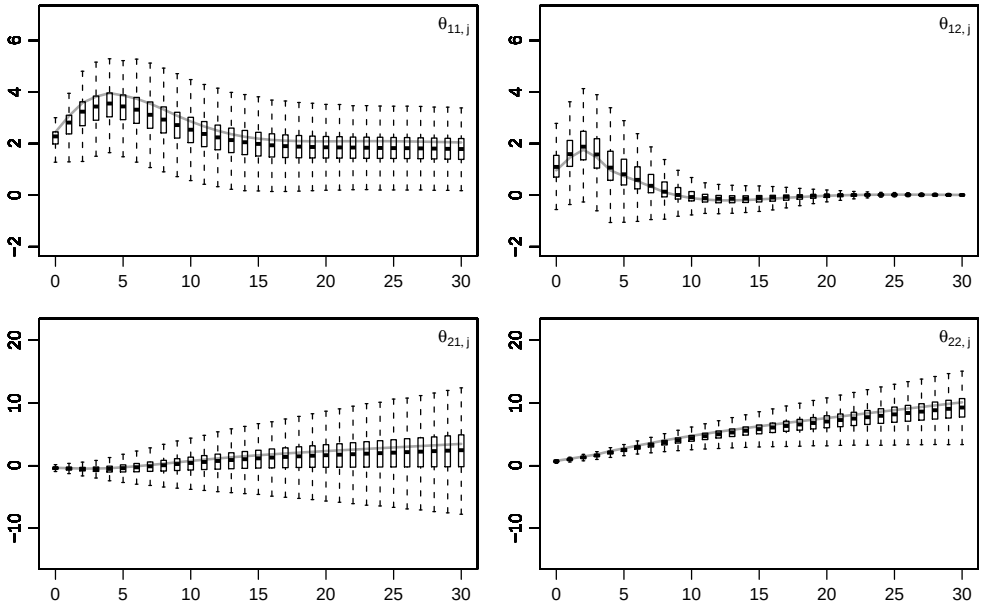

Figure S9: Boxplots of estimated impulse responses based on a FIVAR$_{d_1}$ model with four lags. The solid line shows the true impulse responses from the FIVAR$_b$4 process (S10) of which 5000 replications with 250 observations were drawn

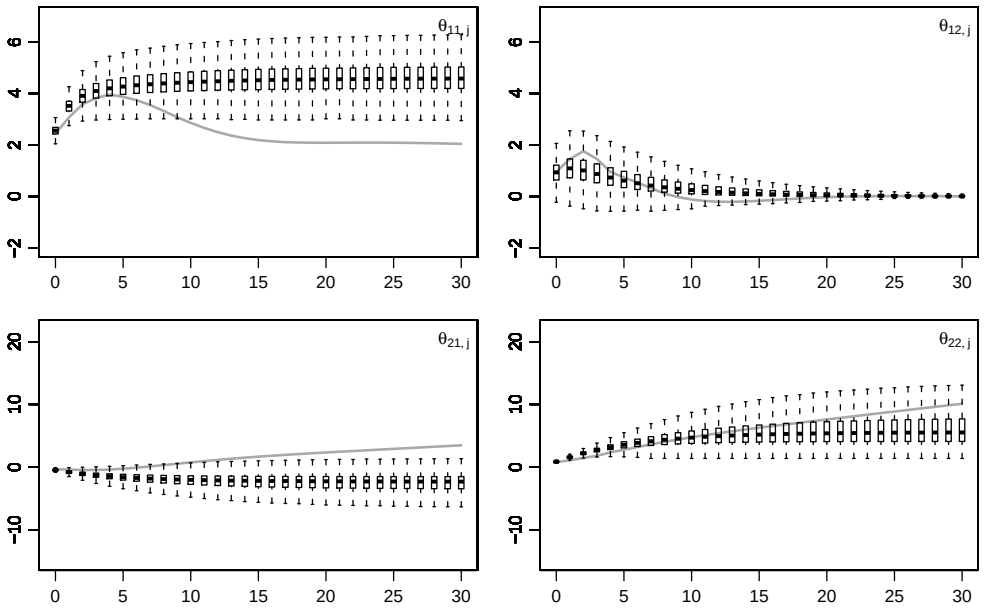

Figure S10: Boxplots of estimated impulse responses based on an IVAR(1,1) model with one lag. The solid line shows the true impulse responses from the FIVAR$_b$4 process (S10) of which 5000 replications with 250 observations were drawn

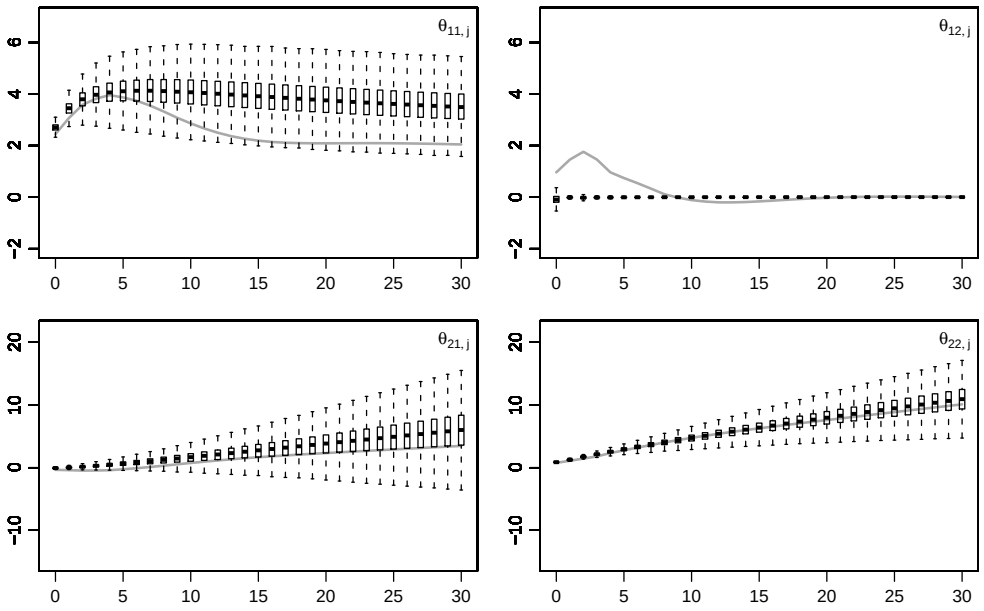

Figure S11: Boxplots of estimated impulse responses based on a FIVAR$_{d_1}$ model with one lag. The solid line shows the true impulse responses from the FIVAR$_b$4 process (S10) of which 5000 replications with 250 observations were drawn

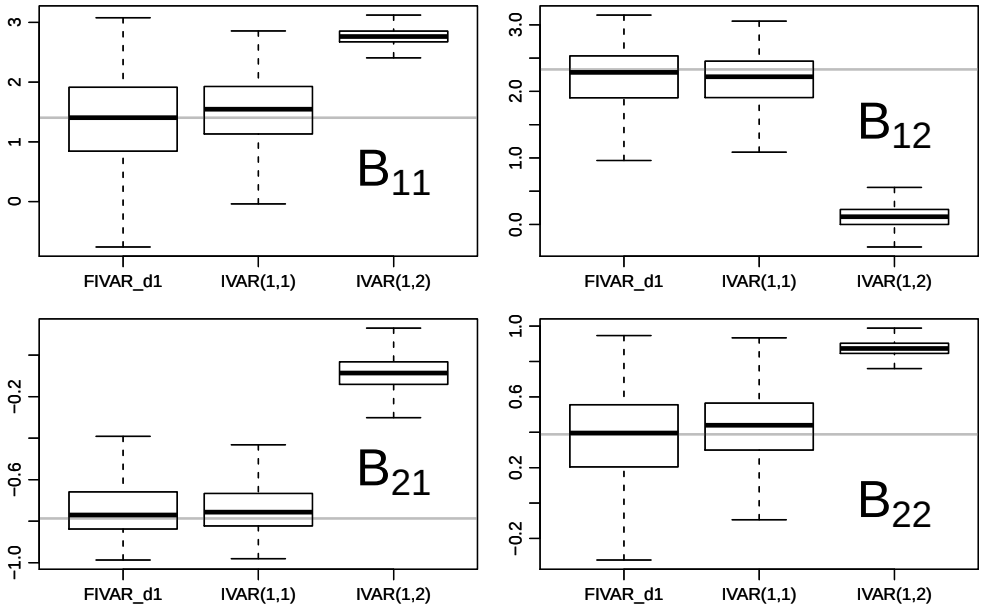

Figure S12: Boxplots of estimated impact coefficients. The true process is given by IVAR1 (S11) of which 5000 replications with 250 observations were drawn.

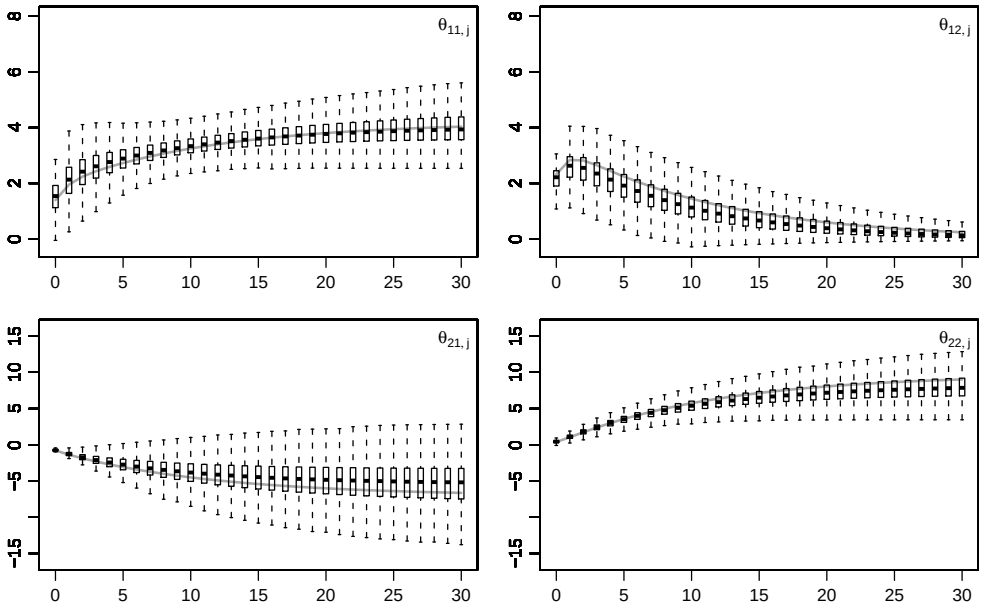

Figure S13: Boxplots of estimated impulse responses based on an IVAR(1,1) model with one lag. The solid line shows the true impulse responses from the IVAR1 process (S11) of which 5000 replications with 250 observations were drawn

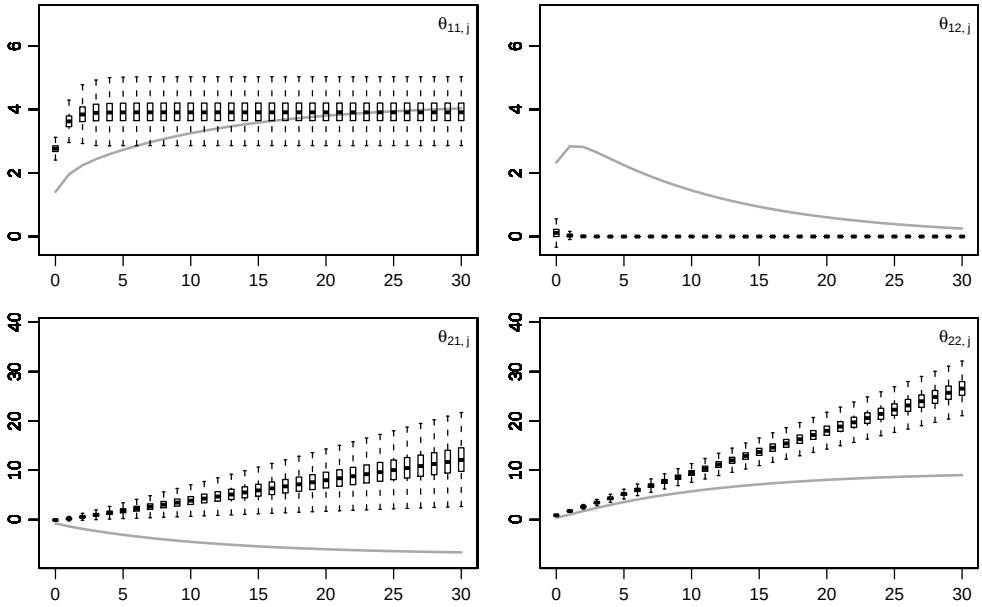

Figure S14: Boxplots of estimated impulse responses based on an IVAR(1,2) model with one lag. The solid line shows the true impulse responses from the IVAR1 process (S11) of which 5000 replications with 250 observations were drawn

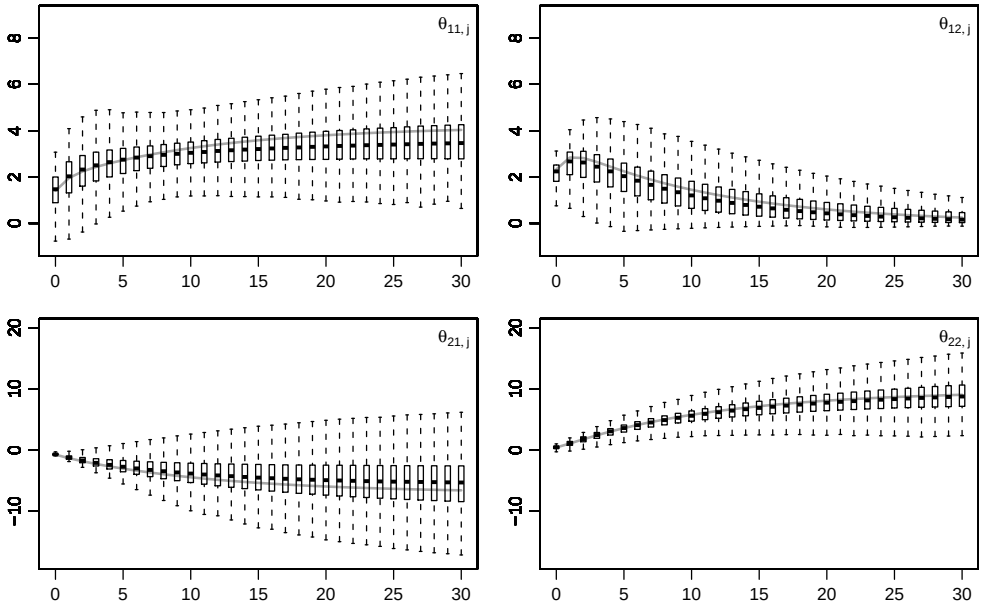

Figure S15: Boxplots of estimated impulse responses based on a FIVAR_{d_1} model with one lag. The solid line shows the true impulse responses from the IVAR1 process (S11) of which 5000 replications with 250 observations were drawn

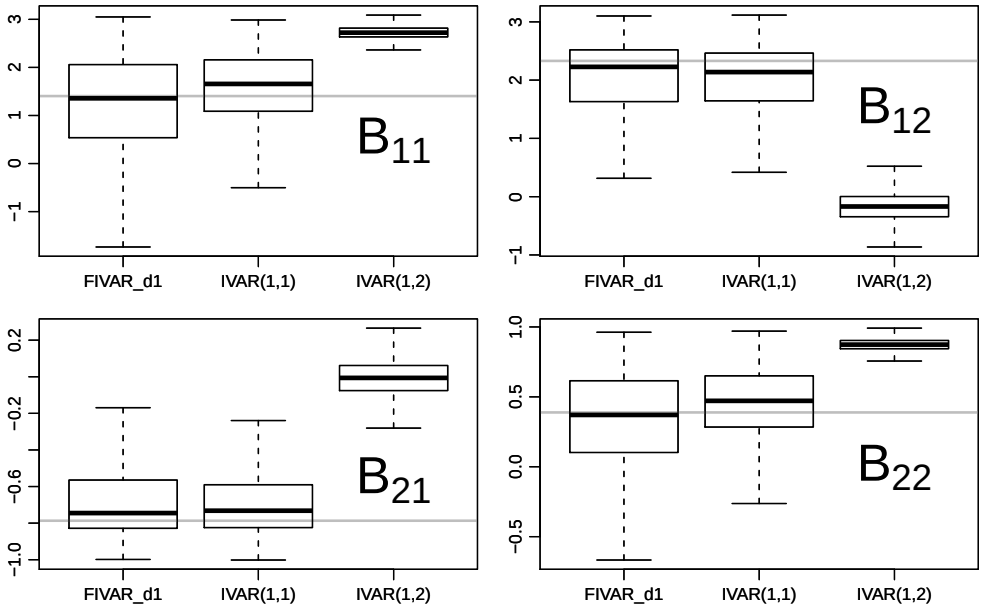

Figure S16: Boxplots of estimated impact coefficients. The true process is given by IVAR4 (S12) of which 5000 replications with 250 observations were drawn.

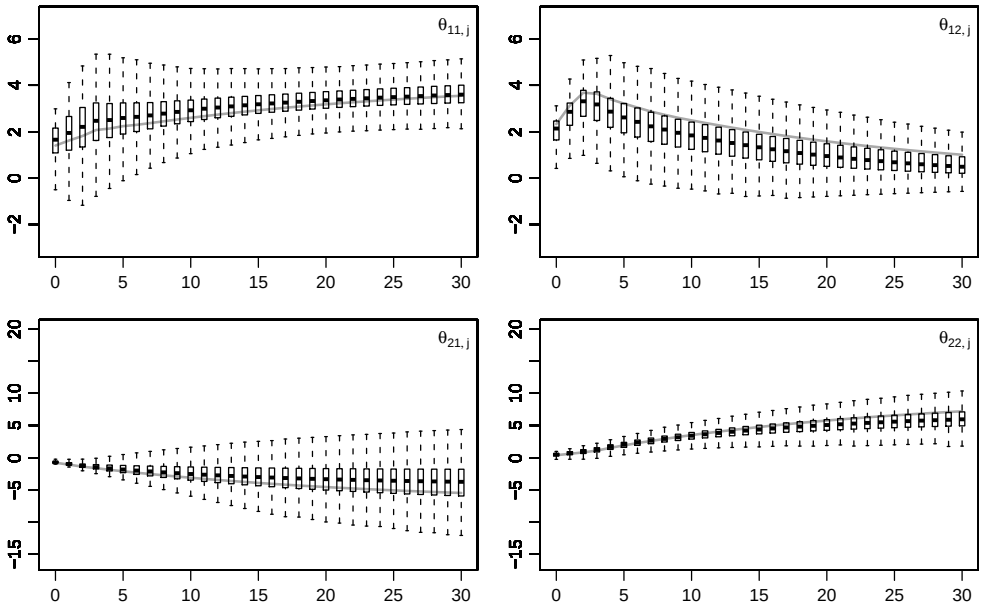

Figure S17: Boxplots of estimated impulse responses of an IVAR(1,1) model with four lags. The solid line shows the true impulse responses from the IVAR4 process (S12) of which 5000 replications with 250 observations were drawn

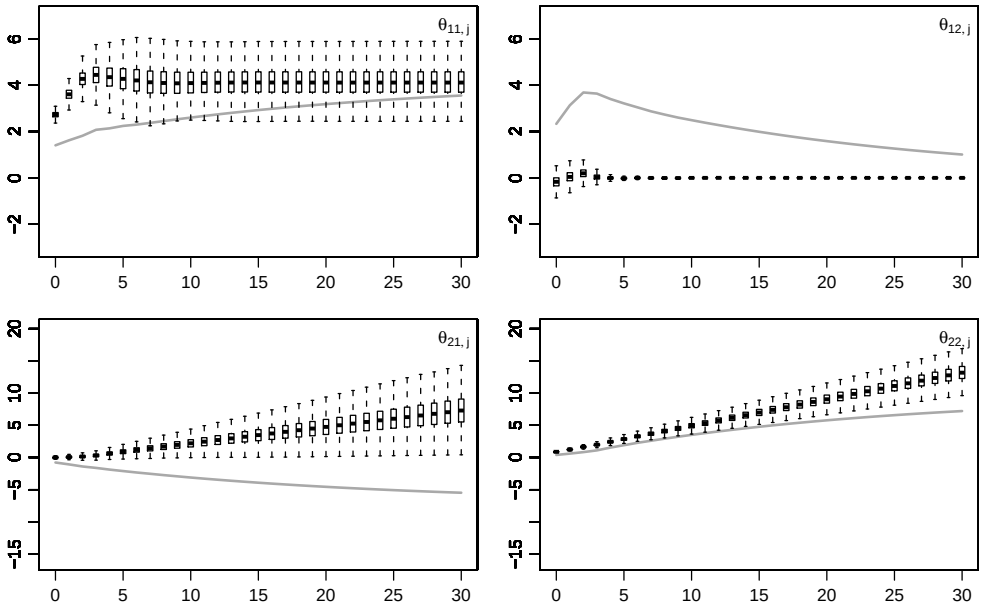

Figure S18: Boxplots of estimated impulse responses of an IVAR(1,2) model with four lags. The solid line shows the true impulse responses from the IVAR4 process (S12) of which 5000 replications with 250 observations were drawn

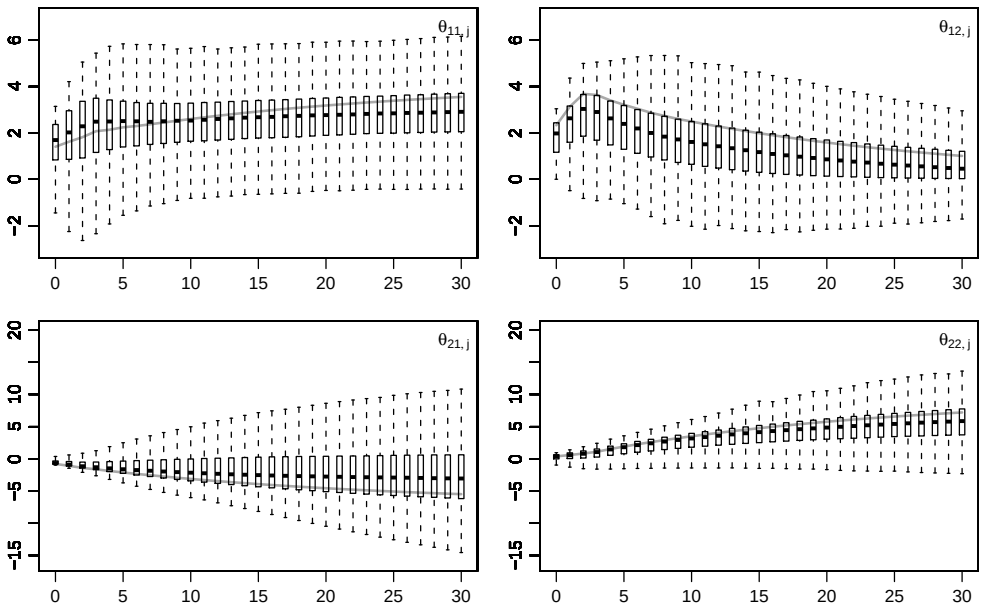

Figure S19: Boxplots of estimated impulse responses of a FIVAR$_{d_1}$ model with four lags. The solid line shows the true impulse responses from the IVAR4 process (S12) of which 5000 replications with 250 observations were drawn

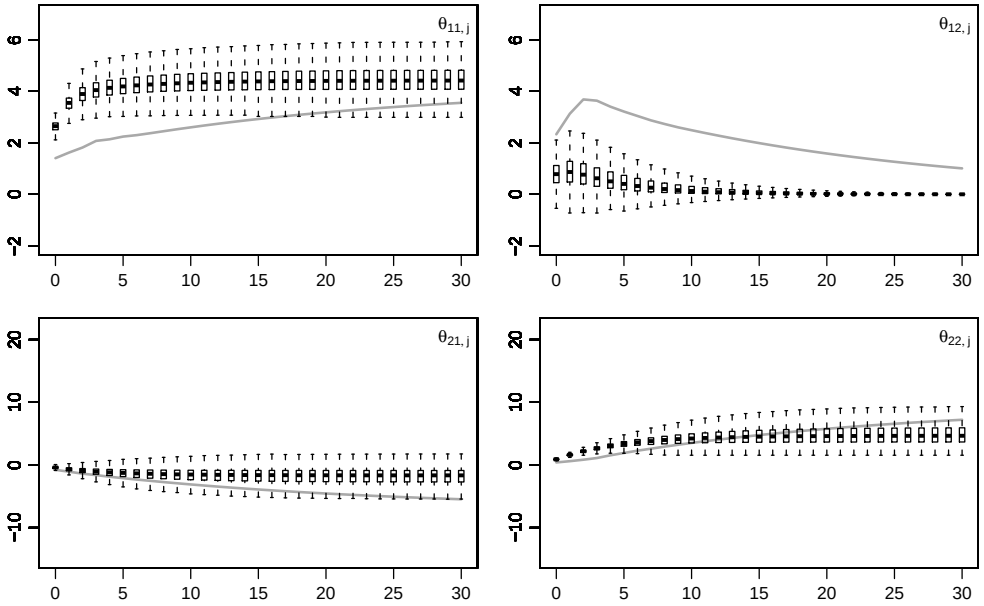

Figure S20: Boxplots of estimated impulse responses of an IVAR(1,1) model with one lag. The solid line shows the true impulse responses from the IVAR4 process (S12) of which 5000 replications with 250 observations were drawn

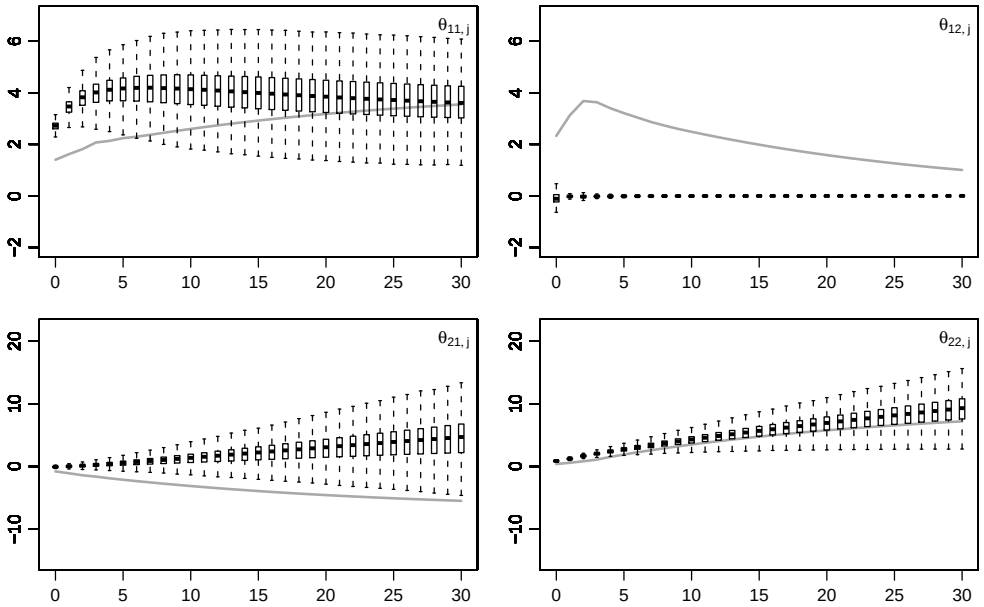

Figure S21: Boxplots of estimated impulse responses of a FIVAR_{d_1} model with one lag. The solid line shows the true impulse responses from the IVAR4 process (S12) of which 5000 replications with 250 observations were drawn

REFERENCES

Chung, C. (2001), "Calculating and Analyzing Impulse Responses for the Vector ARFIMA Model." *Economics Letters*, 71, 17 – 25.

Davidson, J. (1994), *Stochastic Limit Theory*, Oxford University Press.

Faust, J. (1998), "The Robustness of Identified VAR Conclusions about Money," *Carnegie-Rochester Conference Series on Public Policy*, 49, 207–244.

Gospodinov, N., Maynard, A., and Pesavento, H. (2010), "Sensitivity of Impulse Responses to Small Low Frequency Co-movements: Reconciling the Evidence on the Effects of Technology Shocks," Unpublished Manuscript.

Lütkepohl, H. (1996), *Handbook of Matrices*, Wiley & Sons.

Schotman, P. C., Tschernig, R., and Budek, J. (2008), "Long Memory and the Term Structure of Risk," *Journal of Financial Econometrics*, 2, 1–37.